THE JOURNAL OF BIOLOGICAL CHEMISTRY VOL. 284, NO. 13, pp. 8582–8588, March 27, 2009


# Aromatic Residues ϵTrp-55 and δTrp-57 and the Activation of Acetylcholine Receptor Channels*

Received for publication, September 16, 2008, and in revised form, January 22, 2009 Published, JBC Papers in Press, January 26, 2009, DOI 10.1074/jbc.M807152200

**Pallavi A. Bafna, Archana Jha, and Anthony Auerbach**[1]

*From the Department of Physiology and Biophysics, State University of New York, Buffalo, New York 14214*

**The two transmitter binding sites of the neuromuscular acetylcholine (ACh) receptor channel contain several aromatic residues, including a tryptophan located on the complementary, negative face of each binding pocket. These two residues, Trp-55 in the ϵ subunit and Trp-57 in the δ subunit, were mutated (AEFHILRVY), and for most constructs the rate constants for acetylcholine binding and channel gating were estimated by using single channel kinetic analyses. The rate constants for unliganded channel opening and closing were also estimated for some mutants. From these measurements we calculated all of the equilibrium constants of the "allosteric" cycle as follows: diliganded gating, unliganded gating, dissociation from the C(losed) conformation, and dissociation from the O(pen) conformation. The results indicate the following. (i) These aromatic side chains play a relatively minor role in ACh receptor channel activation. (ii) The main consequence of mutations is to reduce the affinity of the O conformation of the binding site for ACh, with the effect being greater at the ϵ subunit. (iii) In ϵ (but not δ) the aromatic nature of the side chain is important in determining affinity, to a slightly greater degree in the O conformation. Φ value analyses (of both tryptophan residues) show Φ ~1 for both the ACh binding and diliganded gating reactions. (iv) This suggests that the structural boundaries of the dynamic elements of the gating conformational change may not be subunit-delimited, and (v) the mutated tryptophan residues experience energy changes that occur relatively early in both the ligand-binding and channel-gating reactions.**

Acetylcholine receptor channels are allosteric proteins that "gate" the flow of ions at the vertebrate nerve-muscle synapse (1–3). As with other members of this five-subunit ("Cys loop") receptor family, the two AChR[2] agonist-binding sites are located in the extracellular domain of the protein, about 50 Å above the middle of the membrane. The occupancy of these sites by appropriate ligands alters the equilibrium constant for gating, which we define as the global and reversible isomerization of the protein between a stable, low affinity, nonconducting **C** conformation and a stable, high affinity, ion-conducting **O** conformation.

Structures of the heteromeric *Torpedo* muscle-type AChR (4), the homomeric ELIC (5), GLIC (6), and acetylcholine-binding proteins (7, 8) show that each ligand-binding site contains several aromatic residues that are mostly conserved among these pentameric receptors (Fig. 1). In AChRs, residues Tyr-93, Trp-149, Tyr-190, and Tyr-198 are in the $\alpha_\epsilon$ or $\alpha_\delta$ subunit (the positive face of the binding site), and residues Trp-55 and Trp-57 are in the complementary ϵ or δ subunit (the negative face), respectively. The foci of this report are these two minus-side tryptophan residues, which we will refer to as the $W^-$ amino acids.

Affinity labeling studies of AChRs show that the two $W^-$ residues are located near the ACh-binding site and participate in the channel activation process. In *Torpedo*, γTrp-55 and δTrp-57 are sites of photo-incorporation of the competitive antagonist *d*-tubocurarine (9, 10), and γTrp-55 is labeled by the agonist nicotine (11). Also, constitutively active AChRs are formed following the incorporation of a series of tethered quaternary ammonium derivatives at αTrp-149, αTyr-93, and γTrp-55/δTrp-57 (12, 13). These experiments indicate that the $W^-$ residues are close to the agonist-binding site but more distant compared with αTrp-149 and αTyr-93 (for which shorter tethers were effective). Structures of acetylcholine-binding protein confirm this conclusion; the minus-side residue Trp-53 makes limited aromatic contacts with bound ligand, whereas the plus-side aromatic residues Trp-143 and, to a lesser extent, Tyr-185 and Tyr-192 (8), form the main part of an "aromatic box" (14) that surrounds the ligand (Fig. 1, *right*).

To what extents do the $W^-$ side chains influence ligand binding and channel gating? In *Torpedo* AChRs, a leucine substitution at either ϵTrp-55 or δTrp-57 increases the response to $EC_{50}$ and increases the equilibrium dissociation constants for both agonists and antagonists (10). Replacement of Trp-54 in α7 neuronal AChRs (homologous to γTrp-55/δTrp-57 in muscle AChRs) by Phe, Ala, or His produces similar effects (15), as do substitutions at homologous positions in other Cys loop receptors (16–18). At the level of rate and equilibrium constants (estimated by single channel kinetic analysis), the main effect of the mutations ϵW55F and δW57F in mouse AChRs is to slow the forward **C** → **O** rate constant, with more minor effects on the backward **C** ← **O** rate constant and the affinity of the **C** receptor for ACh (19).

Here we extend these single channel studies of the two $W^-$ residues in recombinant $(\alpha 1)_2\beta\delta\epsilon$ mouse AChRs. We examined mutants of these positions and were able to estimate binding, diliganded gating rate, and equilibrium constants for most. Furthermore, for some constructs we also measured the unliganded gating parameters, which allowed us to separately deter-

* This work was supported, in whole or in part, by National Institutes of Health Grant NS-23513. The costs of publication of this article were defrayed in part by the payment of page charges. This article must therefore be hereby marked "*advertisement*" in accordance with 18 U.S.C. Section 1734 solely to indicate this fact.

[1] To whom correspondence should be addressed. Tel.: 716-829-3450; Fax: 716-826-2569; E-mail: auerbach@buffalo.edu.

[2] The abbreviations used are: AChR, acetylcholine receptor; ACh, acetylcholine; WT, wild type.

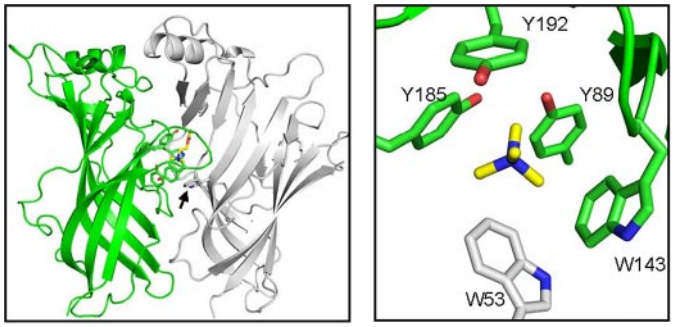


| | A | E | F | H | I | L | R | V | Y |
|---|---|---|---|---|---|---|---|---|---|
| $E_2$ | ●○ | ●○ | ●○ | ○ | ● | ○ | ○ | ●○ | ●○ |
| $K_d$ | ●○ | ● | ●○ | ○ | ● | ○ | ○ | ●○ | ●○ |
| $E_0$ | ●○ | ●○ | ●○ | ○ | ○ | ●○ | ○ | ○ | ●○ |
| $J_d$ | ●○ | ● | ●○ | ○ | | ○ | ○ | ○ | ●○ |

● εW55 ○ δW57

FIGURE 1. **Structure and mutants.** *Top, Lymnaea stagnalis* acetylcholine-binding protein (Protein Data Bank code 1UV6). *Left,* the "plus" subunit is *green,* and the "minus" subunit is *white*. The bound ligand (carbamylcholine, *yellow*) is surrounded by several aromatic residues. The *arrow* marks the $W^-$ residue. *Right,* close-up of the ligand-binding site showing the aromatic residues (≤7 Å from the ligand nitrogen); only the quaternary ammonium moiety of carbamylcholine is displayed. Atom colors: N, *blue*; O; *red*; C *green* (plus subunit), *white* (minus subunit) or *yellow* (ligand). *Bottom,* equilibrium constant measurements for the AChR $W^-$ residues; *circles* indicate that the constant was estimated for that mutant. $E_2$, diliganded gating equilibrium constant; $K_d$, ACh dissociation constant from **C**; $E_0$, unliganded gating equilibrium constant; $J_d$, ACh dissociation constant from **O**.

mine the functional effects of the side chain substitutions on the equilibrium dissociation constants of the **C** *versus* the **O** conformations.

## EXPERIMENTAL PROCEDURES

Detailed methods are given in Jha *et al.* (20). Mutant AChRs were transiently expressed in human embryonic kidney cells, and single channel currents were recorded in the cell-attached patch configuration at 23 °C. The bath and pipette solutions were Dulbecco's phosphate-buffered saline containing (in mM) the following: 137 NaCl, 0.9 $CaCl_2$, 2.7 KCl, 1.5 $KH_2PO_4$, 0.5 $MgCl_2$, and 8.1 $Na_2HPO_4$ (pH 7.3). The currents were digitized at a sampling frequency of 50 kHz. Acetylcholine was added to the pipette solution at concentrations of 30, 100, 300, 500, 1000, 3000, and 5000 μM (Fig. 2). Usually the membrane potential ($V_m$) was approximately −100 mV, but in some experiments at high [ACh] the pipette potential was set to −70 mV ($V_m$ approximately +40 mV) to relieve channel block by the agonist. This voltage perturbation was assumed only to increase the closing rate constant by 10-fold (21).

Rate constant estimation (12 kHz bandwidth) was done by using QUB software. Clusters of individual channel, diliganded **C** ↔ **O** activity were usually selected by eye or by using a critical time of 50 ms (the minimum duration of the intervals flanking a cluster of openings). Clusters produced by εW55R had too low of an open probability for analysis. For all other mutants, the intra-cluster opening and closing rate constants ($n \leq 3$ patches) were estimated from the interval durations by using a maximum likelihood algorithm (22) after imposing a dead time correction of, typically, 50 μs (2.5 samples). In some patches, an additional nonconducting state was connected to the conducting state, to accommodate a component associated with short lived desensitization.

The diliganded opening rate constant ($f_2$) was estimated from the saturation of the "effective" opening rate ($f^*$) profile (Fig. 3). The fitting function was the logistic equation: $f^* = f_2/(1 + e^{s(x-i)})$, where $s$ is the slope, $x$ is [ACh], and $i$ is the inflection concentration. The diliganded closing rate constant ($b_2$) was estimated from the inverse of the open channel lifetime obtained at low ACh concentration (to avoid errors arising from channel block). The diliganded gating equilibrium constant was $E_2 = f_2/b_2$. We could not estimate $f_2$ for the εTrp-55 Cys, His, Leu, and Ser constructs because of insufficient saturation of the dose-response curves.

The ACh association ($k_+$) and dissociation ($k_-$) rate constants were estimated by fitting intra-cluster conducting and nonconducting intervals across two or three different ACh concentrations. Because each $W^-$ mutation was expected to influence only a single binding site, the kinetic Scheme 1 used to fit the interval durations had two equivalent and independent binding sites, where $A$ is the agonist in Scheme 1. In the fitting process, $f_2$ was fixed to the value determined by the method described above, and one association and the corresponding dissociation rate constant were fixed to the wild type values of 167 $\mu M^{-1}\ s^{-1}$ and 24,745 $s^{-1}$ (23). The remaining three free parameters were $k_+^{mut}$, $k_-^{mut}$, and $b_2$.

$\Phi_{gating}$ was estimated as the slope of the rate-equilibrium ($R/E$) plot for gating, which is a log-log plot of $f_2$ *versus* $E_2$ (Fig. 4*A*). $\Phi_{binding}$ was estimated as the slope of the log-log plot of ($k_+^{mut}$) *versus* $k_+^{mut}/k_-^{mut}$ (Fig. 4*B*). The slopes were estimated by an unweighted, linear fit using Origin Pro 7.0.

We attempted to measure unliganded gating (no agonist added to the pipette) in 17 mutant constructs (Ala, Glu, Phe, His, Leu, Arg, Val, and Tyr at εTrp-55 or δTrp-57, plus Ile at δTrp-57). These mutations were expressed on a triple mutant background, either αP272A/αD97A/αY127F (20, 24, 25) or αS269I/αD97A/αY127F (24–26), which by themselves increase the unliganded gating equilibrium constant ($E_0$) by a factor of 2.2 or $1.1 \times 10^6$, respectively and, hence give rise to clusters of unliganded openings (27). We were unable to measure $E_0$ on these backgrounds for two $W^-$ mutants; εW55V exhibited only a high open probability mode, and εW55R did not give rise to unliganded clusters of openings. A spreadsheet of mutants and equilibrium constant measurements is shown in Fig. 1, *bottom.*

## RESULTS

We recorded single channel currents and were able to estimate both ACh binding and diliganded gating rate constants for 13 different $W^-$ mutants. An example analysis of one mutant (εW55F) is shown in Fig. 2. As the concentration of ACh increases, the occupancy of un- and mono-liganded states decreases, and the lifetime of the predominant, slowest intra-cluster nonconducting component becomes briefer. We could estimate a high concentration asymptote for this parameter

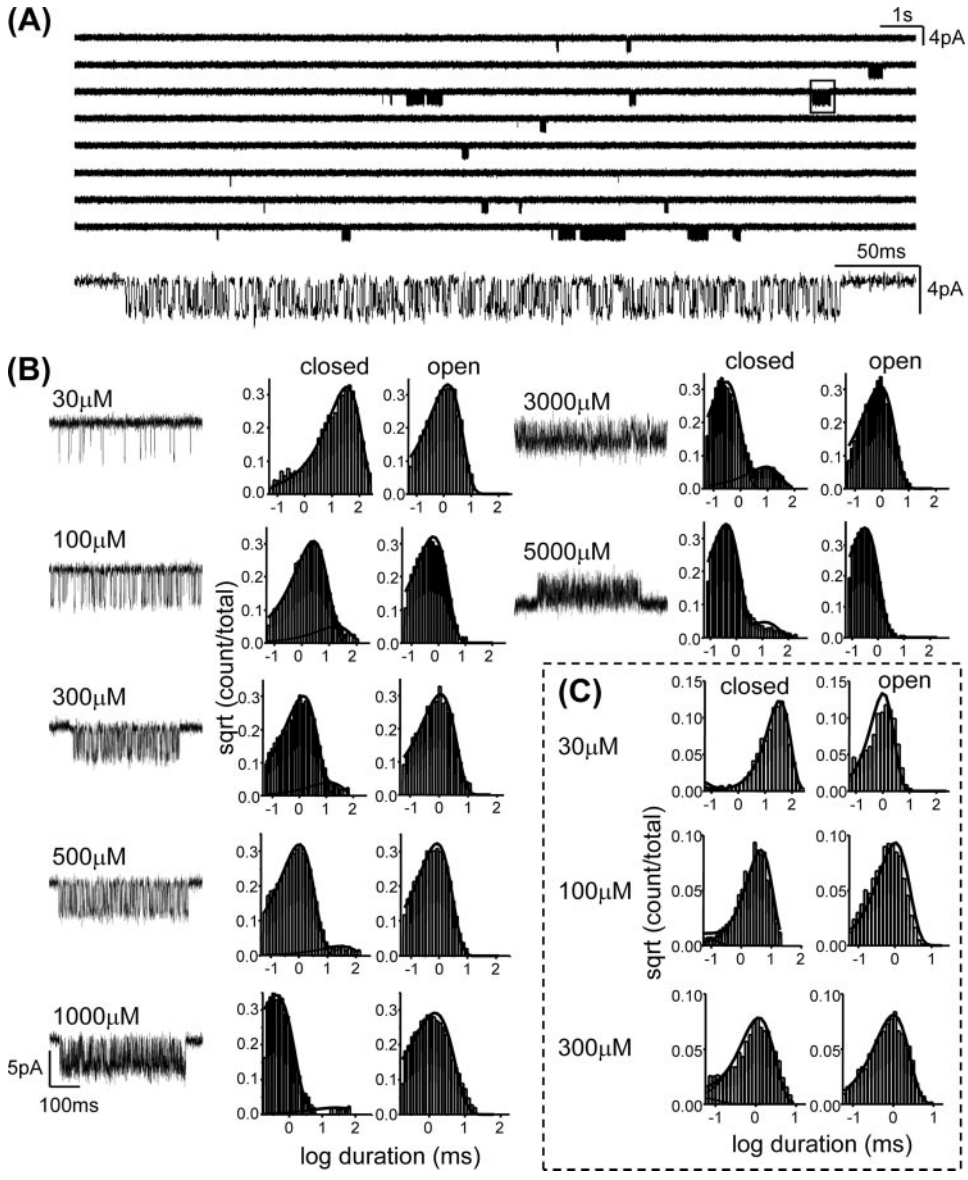


FIGURE 2. **Example single channel kinetic analysis.** *A,* currents from the mutant ϵW55F activated by 500 μM ACh (opening is down). *Top,* low time resolution, continuous current trace; the long shut intervals between clusters of openings are sojourns in desensitized conformations. *Bottom,* expanded view of one cluster (*boxed*); intervals within clusters are diliganded, **C** ↔ **O** gating events. *B,* clusters and interval duration histograms at different [ACh]. The membrane potential was approximately −100 mV except at 5 mM ACh (+40 mV, to relieve channel block). *C,* cross-concentration fitting, to estimate the ACh association and dissociation rate constants. The *solid lines* were calculated from the globally optimized rate constants for all three patches (number of events: 30 μM, 2925; 100 μM, 4545; 300 μM, 5176).

(the inverse of which is an estimate of the diliganded channel opening rate constant) for six ϵTrp-55 mutants and eight δTrp-57 mutants.

The diliganded opening ($f_2$) and closing ($b_2$) rate constants, and their ratio, the diliganded gating equilibrium constant ($E_2$), for these mutant AChRs are shown in Table 1. All of the $W^-$ mutations modestly decreased $E_2$. In ϵ, the largest reductions were for the Ala, Val, and Tyr substitutions (14-fold average reduction), and in δ the largest reductions were for the Arg and Val substitutions (13-fold average reduction). Considering all of the mutations, substitution with regard to $E_2$ was somewhat greater in ϵ (+1.2 kcal $mol^{-1}$) than in δ (+0.7 kcal $mol^{-1}$).

The magnitudes of the effects on $E_2$ are small compared with mutation of other residues in the extracellular domain of the AChR, where side chain substitutions in α (20, 28) and ϵ (29) can reduce diliganded gating by >500-fold (>+3.7 kcal $mol^{-1}$). Perhaps because of the small magnitude of the effect, we could not discern a clear relationship between side chain chemistry and the effect on $E_2$. In the ϵ subunit, the order of $E_2$ magnitude was WI > EF > AVY, and in the δ subunit the order was WEYA > FHL > RV.

At the level of rate constants, the $W^-$ mutations reduced $E_2$ mainly by reducing the channel opening rate constant ($f_2$) rather than increasing the channel closing rate constant ($b_2$). The forward and backward gating rate constants, recast in the form of a rate-equilibrium relationship (*R/E* plot, which is a log-log plot of $f_2$ *versus* $E_2 = f_2/b_2$), are shown in Fig. 4*A*. The slope of this *R/E* plot ($\Phi_{gating}$) for ϵTrp-55 (0.97 ± 0.12; mean ± S.E.) was similar to that for δTrp-57 (0.94 ± 0.11). These values are also indistinguishable from those for agonists (0.93 ± 0.04) (30) or mutations of positive-side position αTrp-149 ((0.87 ± 0.03) (27)). One interpretation of $\Phi_{gating}$ is that it gives (on a scale from 1 to 0) the relative timing of the gating motions of the perturbed residues (early to late) (31, 32). Using this interpretation, this result suggests that the $W^-$ residues experience their **C** *versus* **O** energy change synchronously with each other, as well as with the agonist molecules and residues in the positive face of the binding site, approximately at the onset of the channel opening process.

The equilibrium dissociation constant for ACh binding to the **C** conformation ($K_d$) is the ratio of the (single-site) dissociation/association rate constants ($k_-/k_+$). We were able to estimate these parameters for all of the mutants except Glu and Ile (in δ) and His, Leu, and Arg (in ϵ) (Table 2). All of the side chain substitutions modestly increased $K_d$, on average by ~10-fold (approximately +1.4 kcal $mol^{-1}$). The average effect was approximately equivalent in the ϵ and δ subunits. In ϵ, the aromatic side chains Tyr and Phe caused less of an increase in $K_d$ compared with the nonaromatic side chains, but this pattern was not apparent in δ. The consequence of an Ala substitution was approximately iso-energetic in both subunits.

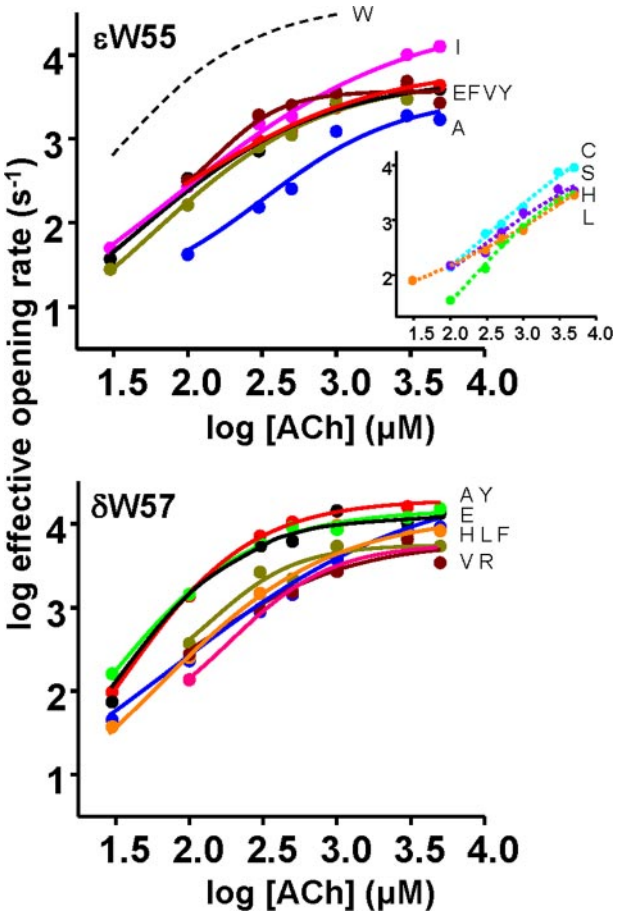


FIGURE 3. **Dose-response curves.** The effective opening rate is the inverse of the predominant (and slowest) intra-cluster nonconducting interval component, whose high concentration asymptote is an estimate of the channel opening rate constant. *Top,* ϵTrp-55 mutations. *W* (WT), *dashed black line* (calculated from the rate constants in Tables 1 and 2); *F*, *black*; *E*, *red*; *A*, *blue*; *I*, *pink*; *V*, *gold*; *Y dark red*. *Inset, C* (*cyan*), *S* (*purple*), *H* (*green*), and *L* (*orange*) mutants showed insufficient saturation to estimate an asymptote. *Bottom,* δTrp-57 mutations. *F*, *black*; *E, red*; *A*, *blue*; *V*, *gold*; Y, *dark red*; *H*, *green*; *L*, *orange*; *R*, *dark pink*.

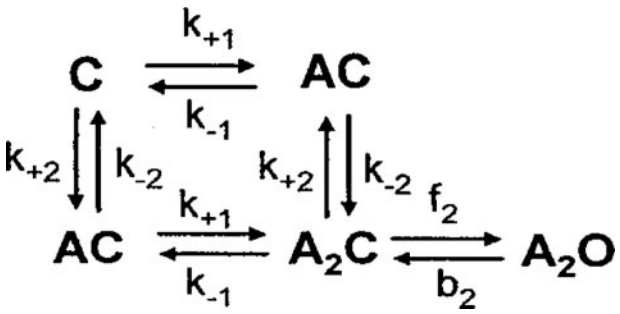


SCHEME 1

The effect of the mutations on $K_d$ was mainly because of a decrease in $k_+$. We next applied *R/E* analysis to the *binding* reaction (**A** + **C** ↔ **AC**), in the same way that we previously applied it to the *gating* reaction (**C** ↔ **O**). The *R/E* plots for the ϵTrp-55 and δTrp-57 ACh binding reactions are shown in Fig. 4*B*, as log-log plots of $k_+$ *versus* $K_a$ (= $1/K_d$). The slopes of these *R/E* curves ($\Phi_{binding}$) were 0.87 ± 0.25 for ϵTrp-55 and 0.89 ± 0.22 for δTrp-57. Despite the large uncertainty, this result suggests that at the transition state for ligand binding the two $W^-$ side chains are mostly "bound-like" in energy (structure), which implies that they change energy relatively early in the **A** + **C** ↔ **AC** binding process.

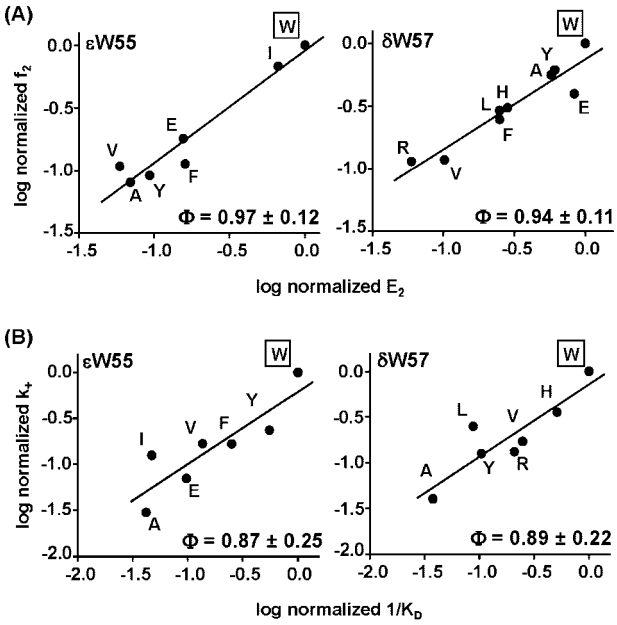


FIGURE 4. ***R/E* plots for diliganded channel gating (*top*) and ACh binding to the C conformation (*bottom*).** The WT side chain is *boxed*. *A,* slope of the gating *R/E* curve ($\Phi_{gating}$) is ~1 for the two $W^-$ positions. This suggests that these residues experience a change in energy (structure) relatively early in the **C** → **O** channel opening process, approximately at the same time as do the agonists and the "+" residue αTrp-149. *B,* slope of the binding *R/E* curve ($\Phi_{binding}$) is ~1 for the two $W^-$ positions. This suggests that these residues move relatively early in the conformational change that accompanies ACh binding to the **C** conformation.

**TABLE 1**

**Diliganded gating parameters**

$f_2$ indicates diliganded opening rate constant; $b_2$ indicates diliganded closing rate constant; $E_2$ indicates diliganded gating equilibrium constant (= $f_2/b_2$); ΔΔ*G* indicates free energy, = $0.59 \cdot \ln(E_2^{WT}/E_2^{mut})$. A positive value indicates that the mutation destabilized **O** relative to **C**.

| Construct | Rate constant | | Equilibrium constant | | |
|---|---|---|---|---|---|
| | $f_2$ | $b_2$ | $E_2$ | Fold change | ΔΔ*G* |
| | $s^{-1}$ | | | | *kcal mol*$^{-1}$ |
| WT[a] | 48,000 | 1700 | 28.2 | | |
| ϵW55A | 3860 | 1970 | 1.9 | 14.4 | +1.6 |
| ϵW55E | 8670 | 1960 | 4.4 | 6.4 | +1.1 |
| ϵW55F | 5440 | 1200 | 4.5 | 6.2 | +1.1 |
| ϵW55I | 32,660 | 1730 | 18.9 | 1.5 | +0.2 |
| ϵW55V | 5190 | 3120 | 1.7 | 17.0 | +1.7 |
| ϵW55Y | 4360 | 1670 | 2.6 | 10.8 | +1.4 |
| δW57A | 29,510 | 1720 | 17.2 | 1.6 | +0.3 |
| δW57E | 19,050 | 810 | 23.6 | 1.2 | +0.1 |
| δW57F | 11,880 | 1690 | 7.0 | 4.0 | +0.8 |
| δW57H | 14,720 | 1830 | 8.0 | 3.5 | +0.7 |
| δW57L | 14,000 | 1990 | 7.0 | 4.0 | +0.8 |
| δW57R | 5490 | 3280 | 1.7 | 16.9 | +1.7 |
| δW57V | 5670 | 1980 | 2.9 | 9.8 | +1.4 |
| δW57Y | 26,910 | 1650 | 16.3 | 1.7 | +0.3 |

[a] Data are from Ref. 39.

In the final series of experiments, we measured the unliganded gating equilibrium constant ($E_0$) for some mutants by using a high, gain-of-function, background construct (Fig. 5). These experiments avoid the problems associated with estimating $E_2$ in the presence of a high [ACh], which under our experimental condition is accompanied by a significant reduction in the single channel current amplitude because of

**TABLE 2**

**ACh binding to the C conformation**

$k_+$ indicates single site association rate constant; $k_-$ indicates single site dissociation rate constant; $K_d$ indicates equilibrium dissociation constant (= $k_-/k_+$) to the **C** conformation; $\Delta\Delta G$, free energy, = $0.59 \cdot \ln(K_d^{mut}/K_d^{WT})$. A positive value indicates that the mutation reduced the affinity of the **C** transmitter binding site for ACh.

| Construct | Rate constant | | Equilibrium constant | | |
|---|---|---|---|---|---|
| | $k_+$ | $k_-$ | $K_d$ | Fold change | $\Delta\Delta G$ |
| | $\mu M^{-1} s^{-1}$ | $s^{-1}$ | $\mu M$ | | *kcal mol*$^{-1}$ |
| WT[a] | 170 | 24,750 | 150[a] | | |
| ϵW55A | 5 | 17,890 | 3740 | 25.3 | +1.9 |
| ϵW55E | 11 | 17,950 | 1610 | 10.8 | +1.4 |
| ϵW55F | 27 | 16,500 | 620 | 4.2 | +0.8 |
| ϵW55I | 20 | 66,310 | 3320 | 22.4 | +1.8 |
| ϵW55V | 27 | 30,640 | 1560 | 10.5 | +1.4 |
| ϵW55Y | 37 | 10,460 | 280 | 1.9 | +0.4 |
| δW57A | 6 | 26,770 | 4170 | 28.1 | +1.9 |
| δW57F[b] | 135 | 30,590 | 230 | 1.5 | +0.2 |
| δW57H | 57 | 17,600 | 310 | 2.1 | +0.4 |
| δW57L | 40 | 70,980 | 1730 | 11.7 | +1.4 |
| δW57R | 21 | 15,570 | 750 | 5.0 | +0.9 |
| δW57V | 27 | 17,160 | 470 | 3.2 | +0.7 |
| δW57Y | 20 | 30,110 | 1510 | 10.2 | +1.3 |

[a] Data are from Ref. 23.
[b] Data are from Ref. 19.

channel block by the agonist. Also, analyses of unliganded gating allowed us to probe the extent to which the change in $E_2$ depends on a change in $E_0$ *versus* the **C** *versus* **O** affinity ratio ($\mathcal{R}$; see under "Discussion").

The results of experiments without any agonist are shown in Table 3. Overall, the $W^-$ substitutions did not have a large effect on $E_0$. In both ϵ and δ, only three substitutions increased $E_0$ by >2-fold. The energy difference between the largest and smallest values of $E_0$ was +1.1 kcal/mol for ϵ55 (Trp-to-His) and +1.6 kcal/mol in δ57 (Leu-to-His). These free energy differences are rather small in comparison with the effect of mutations of positive-side residue αTrp-149, where the energy difference between His *versus* Cys side chains was +3.4 kcal/mol (a 337-fold difference in $E_0$ (27)). Although the $W^-$ mutant unliganded gating energy changes were small, we note that all ϵTrp-55 mutations increased $E_0$, whereas most δ57 mutations decreased $E_0$. This trend implies that without agonists, the relative stability of the **O** *versus* **C** conformation with a Trp is modestly less at position ϵ55, and modestly more at position δ57, compared with most other side chains.

## DISCUSSION

Mutations of the two $W^-$ residues impair ACh binding more than channel gating, but in either case the effects were not particularly large. These aromatic side chains appear to play a relatively minor role in AChR activation. Although other minus-side residues need to be examined, this result suggests that the plus-side of the binding site is the principal structural entity with regard to both ACh binding and channel gating. As far as energy is concerned, the often used phrase describing an AChR-binding site as being "at the interface between subunits" applies to large antagonists (33, 34), but it may be less appropriate in the case of small agonist molecules. All of the ϵTrp-55 and δTrp-57 mutations for which rate and equilibrium constants were estimated reduced $E_2$ and increased $K_d$, which suggests that a Trp at either position is required for the most efficient binding and diliganded gating.

We now quantify the extents to which the magnitudes of $E_2$ in the mutants were determined by the effect of the substitution on the **C** *versus* **O** affinity ratio ($\mathcal{R}$). The AChR is an allosteric protein in which ligand binding and the gating conformational change are coupled energetically (35). Because the $W^-$ mutations change only one of the two binding sites (Equation 1),

$$\mathcal{R}^{mut} = (E_2/E_0)^{mut}/\mathcal{R}^{wt} \quad \text{(Eq. 1)}$$

Using the experimental values for $E_2$ (Table 1) and $E_0$ (Table 3), and the WT value $\mathcal{R}^{WT} = 15{,}600$ (27), we calculate $\mathcal{R}$ values for mutants at the two $W^-$ positions. In the ϵ subunit, the replacement of the Trp (with Ala, Glu, Phe, or Tyr) reduced $\mathcal{R}$, on average, by ~15-fold (Table 4) and increased $E_0$ by ~0.6-fold (Table 3). We conclude that for these constructs, the ~8.5-fold decrease in $E_2$ (Table 1) arises mostly from a decrease in the **C** *versus* **O** affinity ratio. Here, the reduction in $\mathcal{R}$ for nonaromatic side chains was about twice that for aromatic side chains. In the δ subunit the pattern was more complex. For three mutants (Ala, Glu, and Leu), the $\mathcal{R}$ values were approximately the same as in the WT. In the δW57Y construct, the $\mathcal{R}$ value was ~3-fold lower than the WT, and in the remaining four constructs (Phe, His, Arg, and Val), the affinity ratio was ~10-fold lower than the WT. Also, in δ there was no clear distinction between aromatic and nonaromatic side chains. Overall, the effects of $W^-$ mutations on the affinity ratio were greater in ϵ compared with δ.

In WT AChRs the equilibrium dissociation constant of the **O** conformation ($J_d$) is ~10 nM (27). We can calculate $J_d$ for the $W^-$ mutants from the experimental estimates of $K_d$ by using the relationship $\mathcal{R} = K_d/J_d$ (Table 4). For both $W^-$ positions, all of the mutations increased $J_d$ (reduced the **O**-state affinity). The fold increases in $J_d$ were greater than those in $K_d$, except for δW57A and δW57L, where the reductions in affinity were approximately equal in **C** and **O**. We conclude that the main effect of $W^-$ mutations is to specifically reduce the affinity of the **O** conformation of the AChR for the transmitter.

We next consider the effects of $W^-$ mutations on ACh binding to **C** and **O** AChRs in terms of energy. A $\Delta\Delta G$ for ACh binding to the **O** conformation ($J_d$) was calculated for aromatic *versus* nonaromatic side chain substitutions (last column of Table 4). At ϵ55, the (unfavorable) energetic consequence of replacing the Trp with an aromatic side chain (Phe, Tyr; +2.0 kcal/mol) was less compared with replacing with a nonaromatic side chain (Ala, Glu; +3.5 kcal/mol). Similarly, with regard to binding to the **C** conformation ($K_d$; last column of Table 2), the energetic consequence of replacement of Trp with an aromatic side chain (Phe, Tyr; +0.6 kcal/mol) was less compared with replacing with a nonaromatic side chain (Ala, Glu, Ile, and Val; +1.6 kcal/mol). The magnitude of the energy difference between aromatic and nonaromatic was only slightly greater in $J_d$ compared with $K_d$. This implies that at ϵTrp-55, the aromatic nature of the Trp side chain contributes a stabilizing energy of approximately −1.5 kcal/mol for ACh binding to **C**, and approximately −1.0 kcal/mol for binding to **O**. These energies may arise from a cation-π interaction with the ligand, from interactions with residues (or water) on the plus side of the binding site, or both.

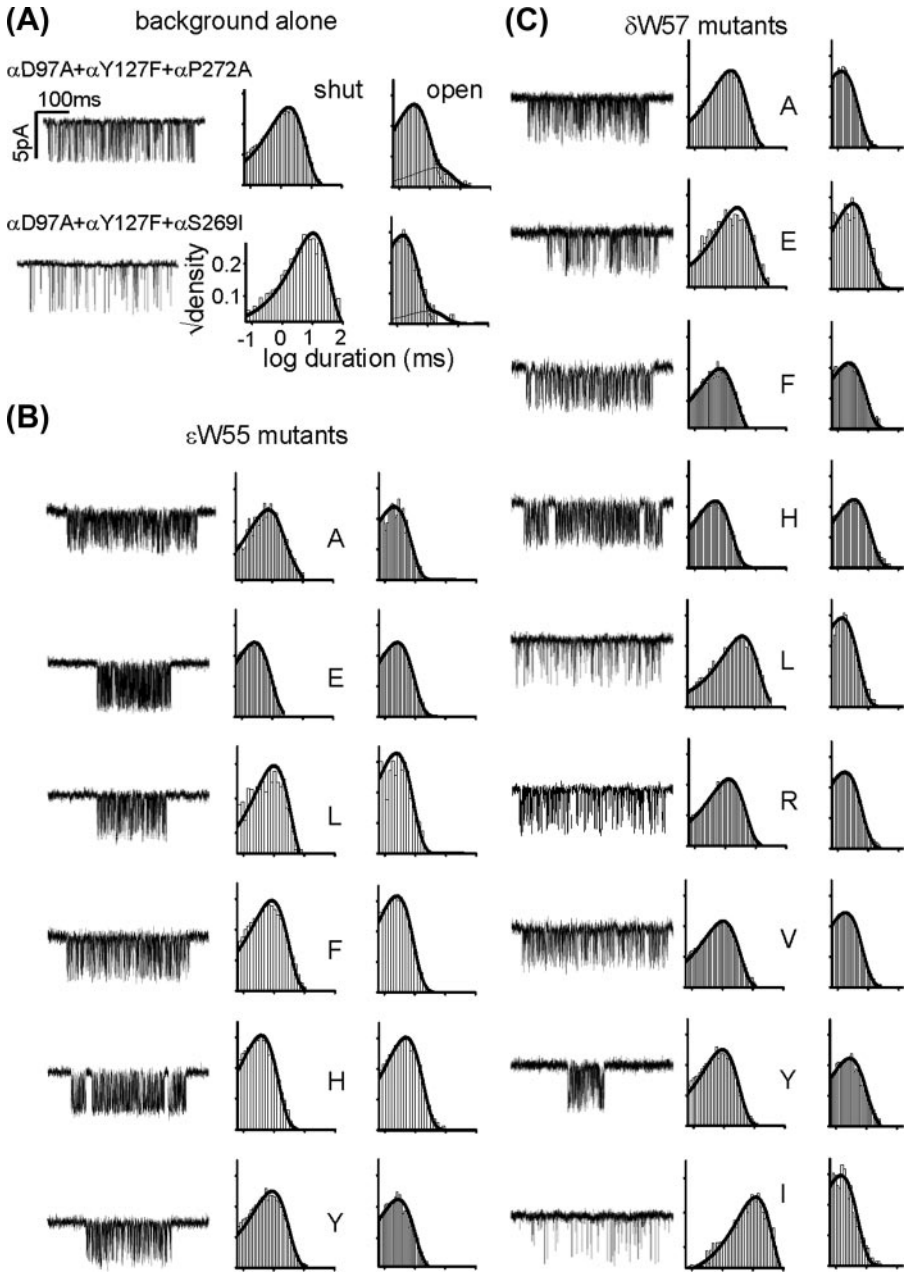


FIGURE 5. **Unliganded gating of W⁻ mutants.** *A,* example clusters and histograms from the two background constructs, without any agonist in the pipette. *B,* unliganded clusters and histograms from the ϵ55 mutants, all expressed on the αD97A/αY127F/αP272A background. *C,* unliganded clusters and histograms from the δ57 mutants, expressed on the αD97A/αY127F/αP272A background except for the Ile construct, which was expressed on the αD97A/αY127F/αS269I background (calibrations as in *A*).

This pattern is not apparent at δ57. Considering all seven mutations here, the excess stabilization of ACh in **O** *versus* **C** was only −0.8 kcal/mol, and with no indication that aromatic side chains provide any more favorable binding energy than nonaromatic side chains, in either the **C** or **O** conformation.

To summarize, at both binding sites W⁻ mutations have a small effect on unliganded gating, a modest effect on binding to the **C** conformation, and a relatively larger effect on binding to the **O** conformation. The ϵTrp-55 residue, and in particular its aromatic nature, plays a more significant role in determining ACh affinity compared with δTrp-57.

Two broader conclusions can be drawn from the Φ value analyses of gating and binding. AChR **C** ↔ **O** gating has been described as a conformational cascade in which nanometer-sized domains ("Φ blocks"), within which all residues undergo their gating structural changes approximately synchronously, move with Brownian dynamics to link the affinity change at the binding site with the conductance change in the pore (31, 36). The $\Phi_{gating}$ values are similar for the residues on both the minus (plus) sides of the subunit interface, including ϵTrp-55 (αTrp-149), δTrp-57 (αTrp-149), and ϵPro-121 (αTrp-149) (29), where Φ ≈1, and δIle-43 (αTyr-127) (28) where Φ ≈0.8. These results raise the possibility that the structural boundaries of Φ blocks may not be delimited by the subunits themselves. Rather, we speculate that the dynamic elements of the conformational cascade (the Φ blocks) span the "quaternary" protein structure.

With regard to binding, the high $\Phi_{binding}$ values for both W⁻ mutant families (Fig. 4*B*) are evidence that the association of ACh to the transmitter binding site is not diffusion-limited, in which case perturbation of $K_d$ should mainly arise from changes in the dissociation rate constant rather than the association rate constant ($\Phi_{binding} \sim 0$). Similarly, high $\Phi_{binding}$ values were found previously for a mutational series of AChR residue αAsp-152 (37), and for different agonists of WT AChRs (where agonist $K_d$ values are mainly determined by the $k_+$ rate constant) (38). Further support for the idea that agonist binding requires a conformational change is that the association rate constant is not diffusion-limited. The smaller agonist, tetramethylammonium ion, associates ~50 times more *slowly* than the larger ACh molecule (38). The experimental observations that agonists and the above-mentioned residues are bound-like in energy at the transition state for binding indicates that there is a conformational change associated with ligand binding, and at this transition state for this reaction (when the channel is still nonconducting) the ligand is in intimate contact with the protein.

The effects of W⁻ mutations on binding and gating are small (compared with mutations of other AChR residues), and in the

**TABLE 3**

**Unliganded gating parameters**

$f_0$ indicates unliganded opening rate constant; $b_0$ indicates unliganded closing rate constant; $E_0$ indicates unliganded gating equilibrium constant; all $W^-$ mutations were expressed on a triple mutant background that increased $E_0^{WT}$ by a factor of $2.2 \times 10^6$ (αD97A/αY127F/αP272A), except for δW57I, which was expressed on a background (αD97A/αY127F/αS269I) that increased $E_0$ by $1.1 \times 10^6$. ΔΔ$G$ indicates free energy, $= 0.59 \cdot \ln(E_2^{WT}/E_2^{mut})$. A positive value indicates that the mutation destabilized **O** relative to **C**.

| Construct | Rate constant | | Equilibrium constant | | |
|---|---|---|---|---|---|
| | $f_0$ | $b_0$ | $E_0$ | Fold change | ΔΔ$G$ |
| | $s^{-1}$ | | | | *kcal mol*$^{-1}$ |
| αD97A/αY127F/αP272A | 840 | 3290 | 0.3 | | |
| αD97A/αY127F/αS269I | 190 | 3990 | 0.1 | | |
| +ϵW55A | 1830 | 5760 | 0.3 | 1.3 | −0.2 |
| +ϵW55E | 5290 | 5340 | 1.0 | 4.0 | −0.8 |
| +ϵW55F | 2320 | 4840 | 0.5 | 1.9 | −0.4 |
| +ϵW55H | 3840 | 2390 | 1.6 | 6.4 | −1.1 |
| +ϵW55L | 1820 | 5320 | 0.3 | 1.4 | −0.2 |
| +ϵW55Y | 2140 | 7310 | 0.3 | 1.2 | −0.1 |
| +δW57A | 1080 | 8320 | 0.1 | 0.5 | +0.4 |
| +δW57E | 530 | 3600 | 0.1 | 0.6 | +0.3 |
| +δW57F | 1720 | 4090 | 0.4 | 1.7 | −0.3 |
| +δW57H | 2700 | 3570 | 0.8 | 3.0 | −0.7 |
| +δW57I | 130 | 7550 | 0.0 | 0.4 | +0.5 |
| +δW57L | 390 | 7410 | 0.1 | 0.2 | +1.0 |
| +δW57R | 1130 | 6480 | 0.2 | 0.7 | +0.2 |
| +δW57V | 1300 | 5180 | 0.3 | 1.0 | 0.0 |
| +δW57Y | 1940 | 4440 | 0.4 | 1.8 | −0.3 |

**TABLE 4**

**Affinity ratio and ACh binding to the O conformation**

$\mathcal{R}$ indicates the **C** *versus* **O** affinity ratio ($= K_d/J_d$); ΔΔ$G$ indicates free energy, $= 0.59 \cdot \ln(\mathcal{R}^{mut}/\mathcal{R}^{WT})$. A positive value indicates that the mutation decreased $\mathcal{R}$. $J_d$ indicates equilibrium dissociation constant for ACh binding to the **O** conformation; ΔΔ$G$ indicates free energy $0.59 \cdot \ln(J_d^{mut}/J_d^{WT})$. A positive value indicates that the mutation reduced the affinity of the **O** transmitter binding site for ACh.

| Construct | Affinity ratio | | | Equilibrium constant | | |
|---|---|---|---|---|---|---|
| | $\mathcal{R}$ | Fold change | ΔΔ$G$ | $J_d$ | Fold change | ΔΔ$G$ |
| | | | *kcal mol*$^{-1}$ | nM | | *kcal mol*$^{-1}$ |
| WT | 15,600 | | | 10 | | |
| ϵW55A | 860 | 0.1 | +1.7 | 4330 | 433 | +3.6 |
| ϵW55E | 630 | 0.0 | +2.0 | 2560 | 256 | +3.3 |
| ϵW55F | 1330 | 0.1 | +1.5 | 470 | 47 | +2.3 |
| ϵW55Y | 1270 | 0.1 | +1.5 | 220 | 22 | +1.8 |
| δW57A | 18,660 | 1.2 | −0.1 | 220 | 22 | +1.8 |
| δW57E | 22,170 | 1.4 | −0.2 | | | |
| δW57F | 2360 | 0.2 | +1.1 | 100 | 10 | +1.3 |
| δW57H | 1490 | 0.1 | +1.4 | 210 | 21 | +1.8 |
| δW57L | 19,830 | 1.3 | −0.1 | 90 | 8 | +1.3 |
| δW57R | 1390 | 0.1 | +1.4 | 540 | 54 | +2.4 |
| δW57V | 1620 | 0.1 | +1.3 | 290 | 29 | +2.0 |
| δW57Y | 5230 | 0.3 | +0.6 | 290 | 29 | +2.0 |

absence of high resolution structures of both the apo and liganded neuromuscular AChR, we cannot speculate on the origins of the energy differences we have quantified. However, we hope that in the future our experimental estimates can be used, along with structural and computational results, to identify the precise sources of the energy changes caused by $W^-$ mutations. In addition, the mutants we have studied may some day prove to be useful with regard to engineering the AChR transmitter-binding site.

*Acknowledgments—We thank M. Teeling, M. Merritt, and M. Shero for technical assistance.*

**REFERENCES**


1. Karlin, A. (1977) *Methods Enzymol.* **46,** 582–590
2. Sine, S. M., and Engel, A. G. (2006) *Nature* **440,** 448–455
3. Unwin, N. (1998) *J. Struct. Biol.* **121,** 181–190
4. Unwin, N. (2005) *J. Mol. Biol.* **346,** 967–989
5. Hilf, R. J., and Dutzler, R. (2008) *Nature* **452,** 375–379
6. Bocquet, N., Nury, H., Baaden, M., Le Poupon, C., Changeux, J. P., Delarue, M., and Corringer, P. J. (2009) *Nature* **457,** 111–114
7. Brejc, K., van Dijk, W. J., Klaassen, R. V., Schuurmans, M., van Der Oost, J., Smit, A. B., and Sixma, T. K. (2001) *Nature* **411,** 269–276
8. Celie, P. H., van Rossum-Fikkert, S. E., van Dijk, W. J., Brejc, K., Smit, A. B., and Sixma, T. K. (2004) *Neuron* **41,** 907–914
9. Chiara, D. C., and Cohen, J. B. (1997) *J. Biol. Chem.* **272,** 32940–32950
10. Xie, Y., and Cohen, J. B. (2001) *J. Biol. Chem.* **276,** 2417–2426
11. Chiara, D. C., Middleton, R. E., and Cohen, J. B. (1998) *FEBS Lett.* **423,** 223–226
12. Li, L., Zhong, W., Zacharias, N., Gibbs, C., Lester, H. A., and Dougherty, D. A. (2001) *Chem. Biol.* **8,** 47–58
13. Stewart, D. S., Chiara, D. C., and Cohen, J. B. (2006) *Biochemistry* **45,** 10641–10653
14. Lester, H. A., Dibas, M. I., Dahan, D. S., Leite, J. F., and Dougherty, D. A. (2004) *Trends Neurosci.* **27,** 329–336
15. Corringer, P. J., Galzi, J. L., Eisele, J. L., Bertrand, S., Changeux, J. P., and Bertrand, D. (1995) *J. Biol. Chem.* **270,** 11749–11752
16. Buhr, A., Baur, R., and Sigel, E. (1997) *J. Biol. Chem.* **272,** 11799–11804
17. Sigel, E., Baur, R., Kellenberger, S., and Malherbe, P. (1992) *EMBO J.* **11,** 2017–2023
18. Yan, D., Schulte, M. K., Bloom, K. E., and White, M. M. (1999) *J. Biol. Chem.* **274,** 5537–5541
19. Akk, G. (2002) *J. Physiol.* (*Lond.*) **544,** 695–705
20. Jha, A., Cadugan, D. J., Purohit, P., and Auerbach, A. (2007) *J. Gen. Physiol.* **130,** 547–558
21. Auerbach, A., Sigurdson, W., Chen, J., and Akk, G. (1996) *J. Physiol.* (*Lond.*) **494,** 155–170
22. Qin, F., Auerbach, A., and Sachs, F. (1997) *Proc. Biol. Sci.* **264,** 375–383
23. Chakrapani, S., Bailey, T. D., and Auerbach, A. (2004) *J. Gen. Physiol.* **123,** 341–356
24. Chakrapani, S., Bailey, T. D., and Auerbach, A. (2003) *J. Gen. Physiol.* **122,** 521–539
25. Purohit, P., and Auerbach, A. (2007) *J. Gen. Physiol.* **130,** 559–568
26. Grosman, C., Salamone, F. N., Sine, S. M., and Auerbach, A. (2000) *J. Gen. Physiol.* **116,** 327–340
27. Purohit, P., and Auerbach, A. (2009) *Proc. Natl. Acad. Sci. U. S. A.* **106,** 115–120
28. Purohit, P., and Auerbach, A. (2007) *J. Gen. Physiol.* **130,** 569–579
29. Ohno, K., Wang, H. L., Milone, M., Bren, N., Brengman, J. M., Nakano, S., Quiram, P., Pruitt, J. N., Sine, S. M., and Engel, A. G. (1996) *Neuron* **17,** 157–170
30. Grosman, C., Zhou, M., and Auerbach, A. (2000) *Nature* **403,** 773–776
31. Auerbach, A. (2005) *Proc. Natl. Acad. Sci. U. S. A.* **102,** 1408–1412
32. Zhou, Y., Pearson, J. E., and Auerbach, A. (2005) *Biophys. J.* **89,** 3680–3685
33. Malany, S., Osaka, H., Sine, S. M., and Taylor, P. (2000) *Biochemistry* **39,** 15388–15398
34. Samson, A., Scherf, T., Eisenstein, M., Chill, J., and Anglister, J. (2002) *Neuron* **35,** 319–332
35. Monod, J., Wyman, J., and Changeux, J. P. (1965) *J. Mol. Biol.* **12,** 88–118
36. Bafna, P. A., Purohit, P. G., and Auerbach, A. (2008) *PLoS ONE* **3,** e2515
37. Zhou, M. (1999) *Molecular Recognition at the Transmitter Binding Site of the Nicotinic Acetylcholine Receptor Channel*. Ph.D. thesis, Department of Physiology and Biophysics, State University of New York, Buffalo, NY
38. Zhang, Y., Chen, J., and Auerbach, A. (1995) *J. Physiol.* (*Lond.*) **486,** 189–206
39. Chakrapani, S., and Auerbach, A. (2005) *Proc. Natl. Acad. Sci. U. S. A.* **102,** 87–92